GEOPHYSICS, VOL. 64, NO. 5 (SEPTEMBER-OCTOBER 1999); P. 1603–1607, 10 FIGS.

Ultrasonic velocity and shear-wave splitting behavior of a Colton sandstone under a changing triaxial stress

Menno W. P. Dillen*, Helma M. A. Cruts‡, Jeroen Groenenboom*, Jacob T. Fokkema*, and Adri J. W. Duijndam*

ABSTRACT

Ultrasonic experiments on a dry Colton sandstone placed in a triaxial pressure machine show that effective stress changes lead to distinct anisotropic velocity changes in compressional waves and shear waves. The stress imprint can be recognized from the associated velocity pattern by relating the velocities to the three normal stress directions. The ultrasonic velocities indicate that the sensitivity of the different waves to stress predominantly depends on stresses applied in the polarization and propagation directions of the particular wave mode. Also, stress-induced changes in shear-wave splitting are observed.

INTRODUCTION

The fact that propagation of elastic waves in rocks can be sensitive to the effective stress has been verified in numerous laboratory experiments (Wyllie et al., 1956; Nur and Simmons, 1969; Tao and King, 1990). In a controlled laboratory experiment the effective stress can be manipulated by changing the pore pressure or, in drained conditions, by changing the applied external stress (Wyllie et al., 1958; Rai and Hanson, 1988). Because the pressure machine we used for the experiments cannot apply a pore pressure, we changed the external stress under dry conditions. A common observation from ultrasonic stress experiments is that induced velocity changes in the stress direction become progressively smaller as stress increases, until an asymptotic value is reached (Wyllie et al., 1956; Nur and Simmons, 1969; Lo et al., 1986). Our experiment is confined to low effective stresses up to 10 MPa where induced velocity changes are most significant. Stress-induced velocity changes can be explained by structural models based on crack geometry and crack density that assume cracks open or close in directions depending on the stress state (Nur, 1971; Hudson, 1980; Crampin, 1982). In this paper, we relate the stress tensor to ultrasonic velocities in a phenomenological way and show how the stress imprint can be recognized from its associated velocity pattern. The data show the velocity change of nine combinations of compressional and shear waves (three propagation and three polarization directions) during a true triaxial stress path. The comparatively large size of the sample and the transducer-sample coupling in our experiments are different from those in previously published experiments. Although the results in this paper are not new, we believe that this experiment produces a unique exposition of data that clarifies the sensitivity of elasto-dynamic waves to stress.

EXPERIMENTAL DESIGN

The ultrasonic experiments (Cruts et al., 1995) were carried out on a cubic block of Colton sandstone. The Colton sandstone formation is an Eocene fluvial deposition located in north-central Utah in the United States. The sample was taken from a channel facies and consists of lithic quartz and feldspar. It is fairly homogeneous and has a porosity of about 13% and an unconfined compressive strength of 47 MPa. After grinding and polishing, the dimensions of the block are $0.205 \times 0.205 \times 0.205\ m^3$.

The block was placed in the triaxial pressure machine in the Rock Mechanics Laboratory at the Delft University of Technology (Figure 1). Each of the three axes of the pressure machine can build up a maximum force of 3500 kN. It is not possible to apply a controlled pore pressure to the rock because it is an open system. The block was greased with petroleum jelly to avoid large shear stresses between the sides of the block and the pressure plates. The loading cycles were applied at a rate of 5 kN/s (0.125 MPa/s).

Three ceramic piezoelectric broad-band transducers with a central frequency of 1 MHz were mounted in each pressure plate. The central transducer is a *P*-wave transducer and the

Manuscript received by the Editor October 7, 1996; revised manuscript received December 17, 1998.
*Delft University of Technology, Faculty of Applied Earth Sciences, Mijnbouwstraat 120, 2628 RX Delft, The Netherlands. E-mail: m.w.p.dillen@ctg.tudelft.nl; J.Groenenboom@mp.tudelft.nl; j.t.fokkema@ta.tudelft.nl; a.j.w.duijndam@ta.tudelft.nl.
‡Shell Research and Technical Services, Volmerlaan 6, 2288 GD Rijswijk, The Netherlands. E-mail: h.m.a.cruts@gabonx.shell.com.

two outer transducers are S-wave transducers. The two shear-wave transducers have perpendicular polarizations aligned along the axis directions. For the shear-wave splitting experiments, the P-wave transducer is exchanged for a diagonally polarized S-wave transducer. Transducers with corresponding polarizations are positioned on opposite sides of the sample. The transducers are in direct contact with the sample and are pressed, with the aid of a spring, with a constant force on the block. Shear-wave couplant was applied to the transducer faces to improve signal quality. Using the transducer-sample coupling configuration described above, a high signal quality was obtained (Groenenboom, 1998).

At zero pressure, the measured P-wave velocities in the X- and Z-directions are approximately equal and differed by 5% from the velocity in the Y-direction. Therefore, we assume that the Colton sandstone has an intrinsic transversely isotropic symmetry, with the symmetry axis aligned in the direction of the Y-axis of the triaxial pressure machine. Equal confining stresses in the X- and Z-directions will therefore preserve the transverse isotropy of the sample, and arbitrary stress patterns will induce an orthorhombic symmetry (Nur, 1971). Figure 2 shows the load cycle $ABCD$ as a function of experiment time. The entire $ABCD$-stress path has equal, normal stresses in the X- and Z-directions. During parts A, B, C, and D, the X-force and the Z-force increase. Part A shows a decrease of the stress in the Y-direction, whereas during parts B and C the stress in the Y-direction was kept constant at 2 MPa and 4 MPa, respectively. Finally, part D simulates increasing hydrostatic stress conditions up to 10 MPa.

EXPERIMENTAL RESULTS

Figure 3 shows the full waveform signals of compressional waves as functions of experiment time (top horizontal axis) and transmission traveltime (vertical axis). The bottom horizontal axis indicates the segments A, B, C, and D similar to those in Figure 2. The source and receiver are both P-wave transducers aligned in the X-direction. The transducer-sample coupling, described in the previous section, produces clean traces with easily discernible first arrivals and amplitudes. To visualize shear-wave splitting, shear-wave transducers were aligned in the X-direction and polarized in the YZ-plane in a direction of 45° to the symmetry axis. Figure 4 displays the waveforms recorded at time intervals during stress pattern $ABCD$. Around the peak stresses of A, B, and C, two distinct waveforms appear and

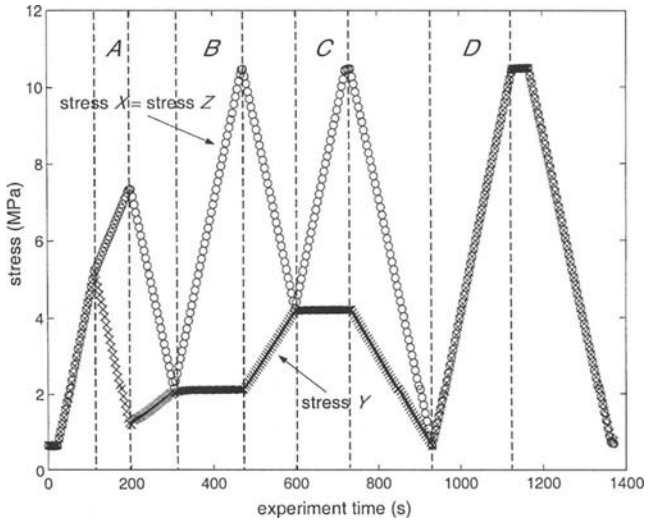

FIG. 2. Loading cycle $ABCD$ of the triaxial pressure machine. To preserve the intrinsic transverse isotropy of the sample, the stress in the X-direction is equal to the stress in the Z-direction.

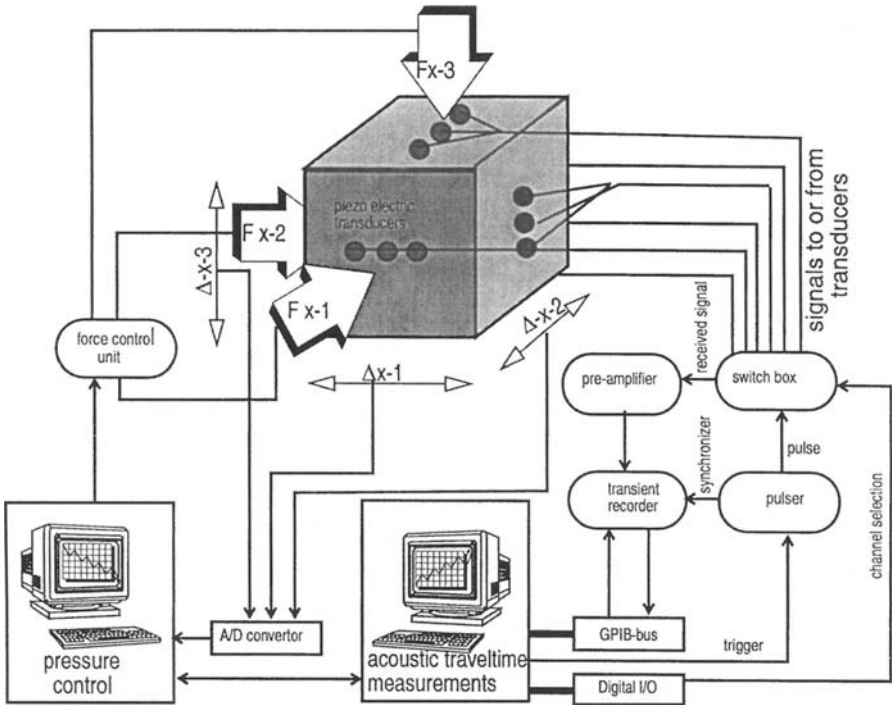

FIG. 1. Schematic layout of the ultrasonic triaxial stress experiment.

again disappear as experiment time progresses. These two distinct waveforms are split shear waves traveling in the same X-direction. Shear-wave splitting becomes visible at those parts of the loading cycle where the stress-induced transverse isotropy is most pronounced. Comparing data from the diagonally polarized transducers with those from transducers polarized in the axis directions, we can determine that the first-arriving shear wave is polarized in the Z-direction and the second-arriving shear wave is polarized in the Y-direction.

From the recordings of P-wave transducer pairs, first arrivals were handpicked, converted to velocities, and displayed in Figure 5. We observe that the P_X- and P_Z-wave velocities (subscript denotes propagation direction) are almost equal and higher than the P_Y-wave velocity during the entire load cycle, reflecting the intrinsic and stress-induced anisotropy of the rock. For part A where the stresses in the X- and Z-directions increase and the stress in the Y-direction decreases, we can see in Figure 5 that the P_X-wave and the P_Z-wave velocities increase and the P_Y-wave velocity decreases. We observe from parts B and C a larger increase of the velocity in the X- and Z-directions than in the Y-direction. In Figure 6, six combinations of shear waves are shown. The S_{XZ} and S_{ZX} shear waves (first subscript denotes propagation direction and second subscript denotes polarization direction) which neither polarize nor propagate in the Y-direction show an overall faster and different velocity behavior than the other four shear-waves, S_{XY}, S_{ZY}, S_{YX}, and S_{YZ}, which either polarize or propagate in the Y-direction.

Figure 7 shows the P_X-wave velocity versus stress. The velocity lines show an approximately linear increase of velocity with stress. The slopes of the lines do not differ much because the stress change in the X- and Z-directions is similar for all four lines. The P_X-wave velocity does not show a clear dependence on the stress changes in the Y-direction. The P_Y-wave stress-velocity pattern in Figure 8 shows a strong dependence on the stress in the Y-direction. P-waves are therefore predominantly affected by the normal component of the stress tensor that lies in the direction of propagation. The 2-D sensitivity of S-waves becomes clear when we look at the S-wave stress-velocity plots. The S_{XZ}-wave velocity plotted in Figure 9 shows no appreciable dependence on the stress change in the Y-direction because of the almost uniform slopes of the velocity lines. We observe

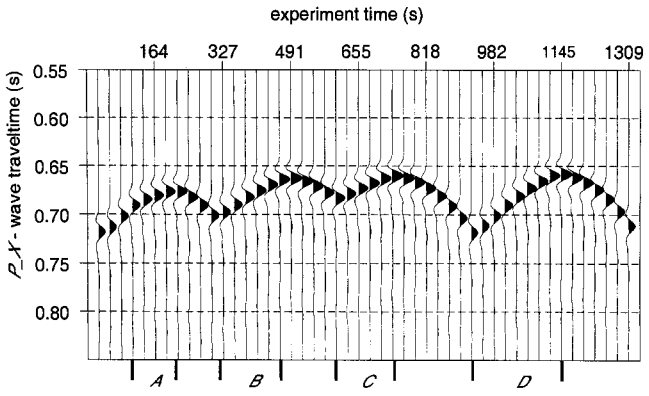

FIG. 3. Ultrasonic recordings of a compressional wave in the X-direction during loadcycle $ABCD$.

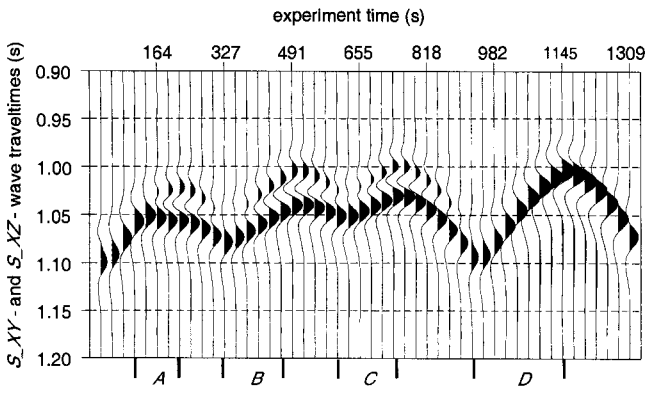

FIG. 4. Shear-wave splitting in the X-direction during load cycle $ABCD$. Transmitting and receiving transducers are positioned diagonally in the YZ-plane.

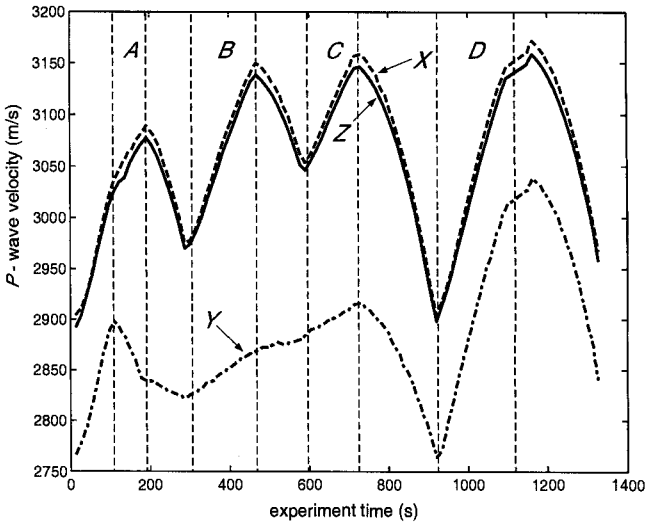

FIG. 5. Velocities of compressional waves propagating in the X-, Y-, and Z-directions during load cycle $ABCD$.

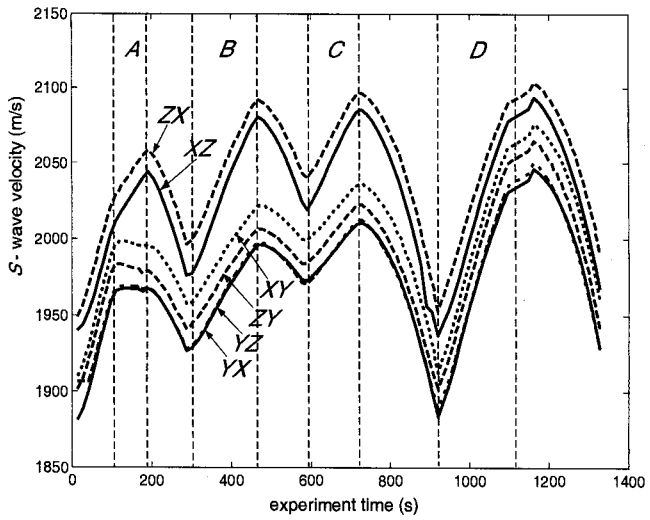

FIG. 6. Velocities of shear waves with propagations (first letter) and polarizations (second letter) in the X-, Y-, and Z-directions during load cycle $ABCD$.

that the stress-velocity pattern of Figure 9 is almost an exact matche to the stress-velocity pattern in Figure 7 because the P_X-wave and the S_{XZ}-wave experience equal stress changes in their propagation and polarization directions. The S_{XY}-wave velocity in Figure 10 shows a stronger dependence on the stress in the Y-direction. However, the correlation with the stress in the Y-direction is less pronounced compared with the stress-velocity pattern observed in Figure 8 for the P_Y-case.

CONCLUSIONS

The experiments on the Colton sandstone described in this paper show how certain changes in a triaxial stress state cause changes in the velocities and anisotropy of compressional and shear waves. We observe that for all applied stress patterns, compressional and shear waves are most sensitive to the normal stresses that lie in the propagation or polarization directions of the wave. Consequently, compressional waves are predominantly sensitive to one direction of the prevailing stress state, whereas shear waves show a 2-D sensitivity to stress. A split shear wave pair is sensitive to all components of the stress tensor. The sensitivity analysis shows how experiments must be designed for acquiring sufficient data in terms of polarization and propagation directions for stress-inference purposes.

ACKNOWLEDGMENTS

This work was funded by the Nederlandse Aardolie Maatschappij B.V. We thank Drs. G. Diephuis for reading the

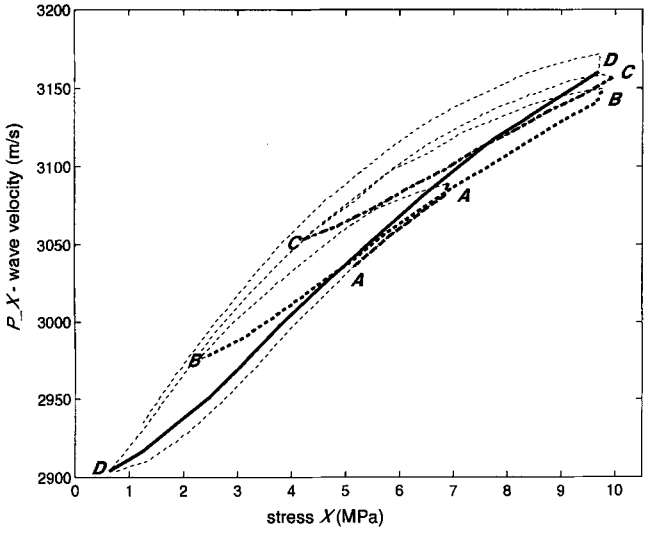

FIG. 7. Velocity of a compressional wave propagating in the X-direction versus the normal stress in the X-direction during load cycle $ABCD$.

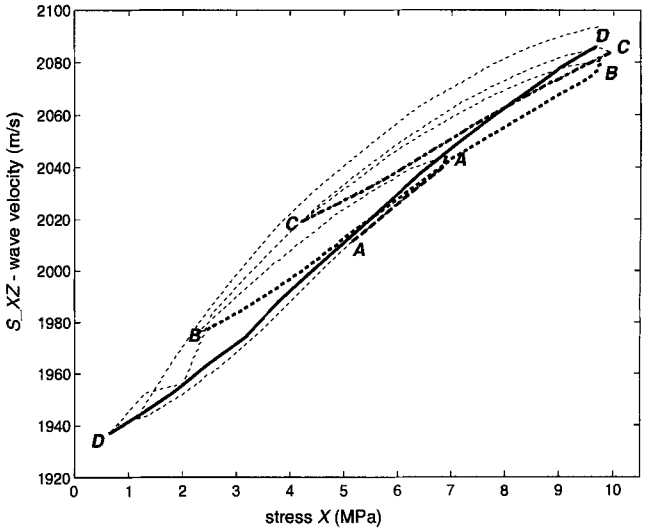

FIG. 9. Velocity of a shear wave with propagation in the X-direction and polarization in the Z-direction versus the normal stress in the X-direction during load cycle $ABCD$.

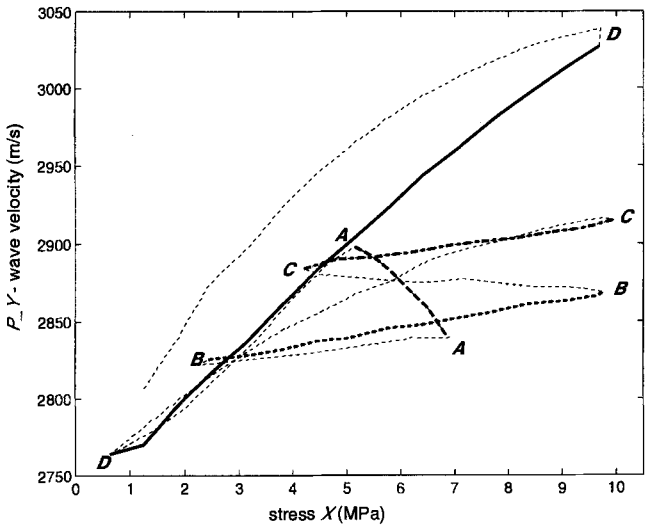

FIG. 8. Velocity of a compressional wave propagating in the Y-direction versus the normal stress in the X-direction during load cycle $ABCD$.

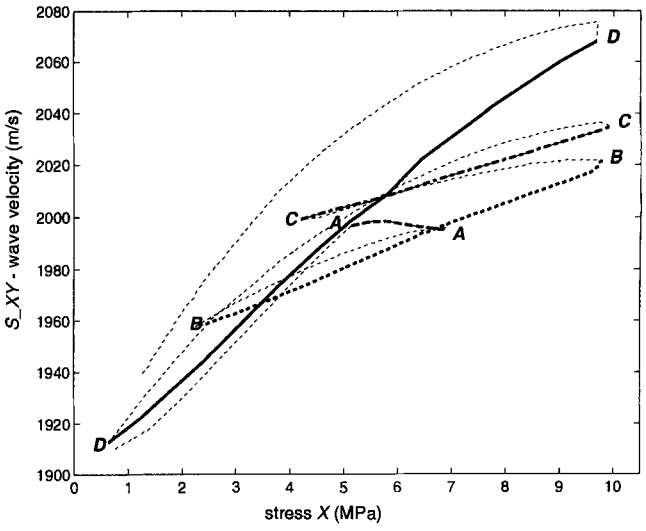

FIG. 10. Velocity of a shear wave with propagation in the X-direction and polarization in the Y-direction versus the normal stress in the X-direction during load cycle $ABCD$.

manuscript and for his comments. The authors acknowlegde D. E. Lumley and an anonymous reviewer for their substantial help in improving this paper.

REFERENCES

Crampin, S., 1982, Effective anisotropic elastic constants for wave propagation through cracked solids: J. Roy. Astr. Soc., **76**, 133–145.

Cruts, H. M. A., Groenenboom, J., Duijndam, A. J. W., and Fokkema, J. T., 1995, Experimental verification of stress-induced anisotropy: 65th Ann. Internat. Mtg., Soc. Expl. Geophys., Expanded Abstracts, 894–897.

Groenenboom, J., 1998, Acoustic monitoring of hydraulic fracture growth: Ph.D. thesis, Delft Univ. of Technology.

Hudson, J. A., 1980, Wave speeds and attenuation of elastic waves in material containing cracks: J. Roy. Astr. Soc., **64**, 133–150.

Lo, T., Coyner, K. B., and Toksöz, M. N., 1986, Experimental determination of elastic anisotropy of Berea sandstone, Chicopee shale, and Chelmsford granite: Geophysics, **51**, 164–171.

Nur, A., and Simmons G., 1969, Stress-induced velocity anisotropy in rock: an experimental study: J. Geophys. Res., **74**, No. 27, 6667–6674.

Nur, A., 1971, Effects of stress on velocity anisotropy in rocks with stress: J. Geophys. Res., **76**, No. 8, 2022–2034.

Rai, C. S., and Hanson, K. E., 1988, Shear-wave velocity anisotropy in sedimentary rocks: A laboratory study: Geophysics, **53**, 800–806.

Tao, G., and King, M. S., 1990, Shear-wave velocity and q anisotropy in rocks: a laboratory study: Int. J. Rock Mech. Min. Sci. and Geomech. Abstr., **27**, No. 5, 353–361.

Wyllie, M. R. J., Gregory, A. R., and Gardner, L. W., 1956, Elastic wave velocities in heterogeneous and porous media: Geophysics, **21**, 41–70.

Wyllie M. R. J., Gregory, A. R., and Gardner, G. H. F., 1958, An experimental investigation of factors affecting elastic wave velocities in porous media: Geophysics, **23**, 459–493.